Soft Semiconductor Devices

RLE Groups
Soft Semiconductor Group, Laboratory of Organic Optics and Electronics

Academic and Research Staff
Professor Marc Baldo

Collaborators
Joseph Shinar[1], Zoltan Soos[2], Nikolai Lebedev[3], Barry Bruce[4], Shuguang Zhang[5]

Postdoctoral Students
Madhusudan Singh

Graduate Students
Mihail Bora, Kemal Celabi, Benjie Limketkai, Jonathan Mapel, Kaveh Milaninia, Michael Segal

Support Staff
George Hall

Introduction

Our group works with soft semiconductors. These are materials comprised of molecules held together by weak *van der Waals* bonds. In comparison, the atoms in conventional semiconductors are held together by strong *covalent* bonds. Weak intermolecular bonds offer a tradeoff to engineers. Their disadvantage is an enhancement of disorder and charge localization, yielding relatively poor charge transport properties.

But the advantage of soft semiconductors is that they are uniquely suited for large area electronics such as video displays, and solar cells. In contrast with the painstaking growth requirements of conventional semiconductors, films of soft semiconductors are readily deposited on a variety of materials at room temperature. Most importantly, the optical properties of the molecules within a soft semiconductor are relatively immune to structural defects and disorder in the bulk. Thus, soft semiconductors are tolerant of the defects that inevitably occur in the fabrication of large area applications.

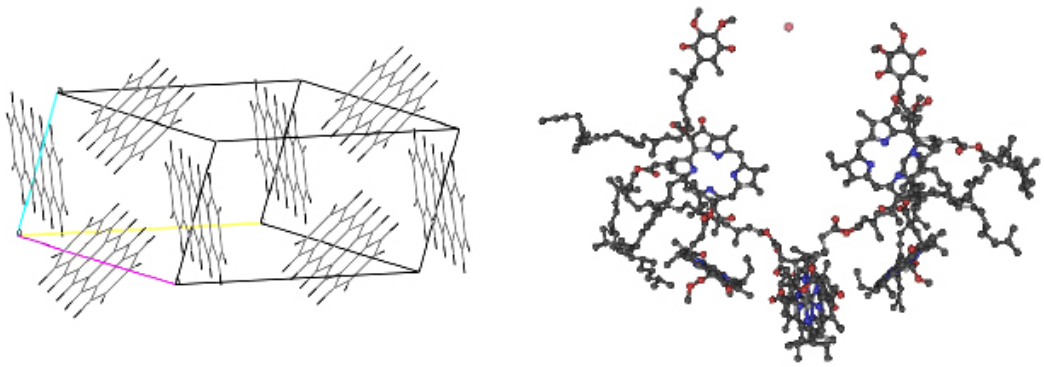

Fig. 1. Two examples of van der Waals bonded semiconductors. **(left)** The structure of a molecular crystal of pentacene. Pentacene has a hole mobility of approximately 2 cm^2/Vs and is widely used in organic electronics. Data is from Mattheus, et al. Acta Crystallographica C. **57**, 939 (2001). **(right)** The structure of the photosynthetic reaction center of Rhodobacter sphaeroides. Evolved over two billion years, this molecular circuit is the backbone of photosynthesis. The protein scaffold has been removed for clarity. Data is from Ermler, et al. Structure **2**, 925 (1994).

[1] Ames Laboratory and Physics and Astronomy Department, Iowa State University
[2] Department of Chemistry, Princeton University
[3] Center for Bio/Molecular Science and Engineering, U.S. Naval Research Laboratory
[4] Department of Biochemistry, Cellular and Molecular Biology, University of Tennessee
[5] Center for Biomedical Engineering, MIT

Biological electronics is the other main application for soft semiconductors. In biology, complex circuits are fabricated by 'bottom-up' self-assembly from molecular components. For example, photosynthesis relies on self-assembled complexes of a handful of weakly interacting molecules positioned by a protein scaffold. These structures are perhaps the smallest electronic circuits known. But they harvest photons with nearly 100% quantum yield and an expected power conversion efficiency exceeding 20%. Biological photosynthetic complexes are perhaps the ultimate demonstration of the promise of soft semiconductors.

This is a young field, with much promise and significant challenges. In our work, we have successfully integrated complex structures from photosynthesis with solid-state electronics. We also work in two of the major controversies in thin film soft semiconductors: the fundamental efficiency limit of organic light emitting devices, where we have questioned accepted models of excited-state formation; and charge injection, where we have developed a theory centered on structural and energetic disorder in these soft materials.

1. Solid State Integration of Photosynthetic Protein Molecular Complexes

Sponsors
DARPA/AFOSR F49620-02-1-0399, National Science Foundation NIRT

Project Staff
Jonathan Mapel, Madhusudan Singh, Michael Segal, Professor Marc Baldo

Over two billion years of evolutionary adaptation have optimized the functionality of biological photosynthetic complexes. Plants and photosynthetic bacteria, for example, contain protein molecular complexes that harvest photons with nearly optimum quantum yield and an expected power conversion efficiency exceeding 20%.

We have demonstrated the solid state integration of photosynthetic complexes. The functionality of the complexes is tested by fabricating solid state photodetectors and photovoltaic devices, using complexes isolated from spinach leaves or photosynthetic bacteria. The internal quantum efficiency of the first generation of devices is estimated to be 12% [1].

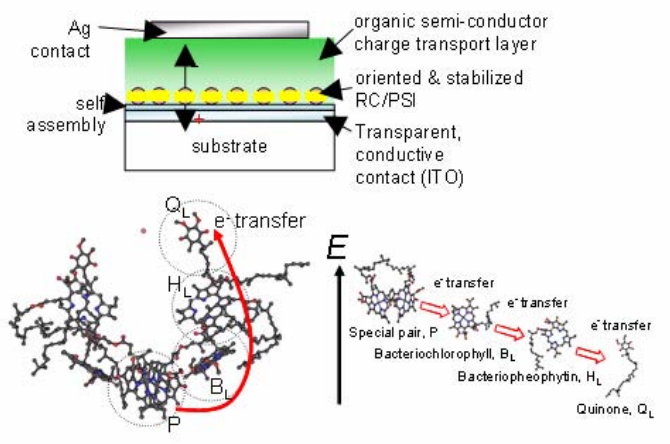

Figure 1: (top left) The structure of solid-state devices incorporating photosynthetic complexes. **(bottom left)** The internal molecular circuitry of a photosynthetic bacterial reaction center with the protein scaffold removed for clarity. The complex is only a few nanometers top-to-bottom. After photoexcitation, an electron is transferred from the special pair, P, to the quinone, Q_L. The process occurs within 200ps, at nearly 100% quantum efficiency, and results in a 0.5V potential across the complex.

Stabilizing the complexes in an artificial environment is the key barrier to successful device integration [2]. We achieved electronic integration of devices (see Fig. 1) by stabilizing an oriented, self-assembled monolayer of photosynthetic complexes using novel surfactant peptides, and then depositing an organic semiconducting protective coating, required as a buffer to prevent damage to the complexes when depositing the top metal contact. Successful integration is conclusively demonstrated by comparisons of the absorption spectrum and photocurrent spectra in Fig. 2.

While initial results demonstrate the functionality of biological materials in solid state devices, photovoltaic performance is limited due to low light absorption; monolayers of photosynthetic structures absorb < 1% of incident light, leading to low overall power efficiencies.

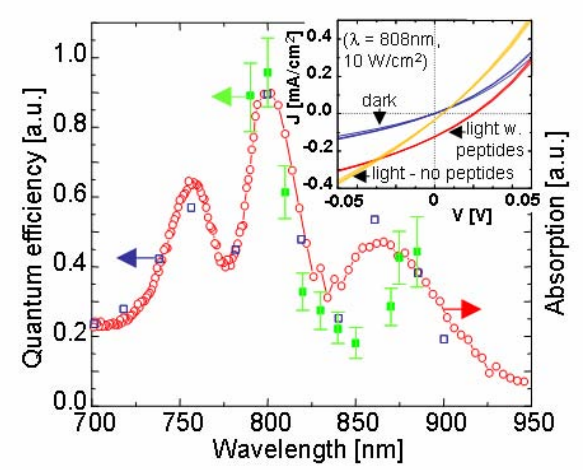

Figure 2: The photocurrent spectrum of solid-state photovoltaic devices employing bacterial reaction centers (RCs). A comparison between the photocurrent spectrum of solid-state (■) and wet electrochemical cell devices (□), and the solution absorption spectrum of the bacterial reaction centers (–o–), demonstrates that the observed photocurrent originates in the RCs. **Inset**: stabilization of RC complexes with A_6K/V_6D peptides improves the internal quantum efficiency of the devices to 12% under short circuit conditions.

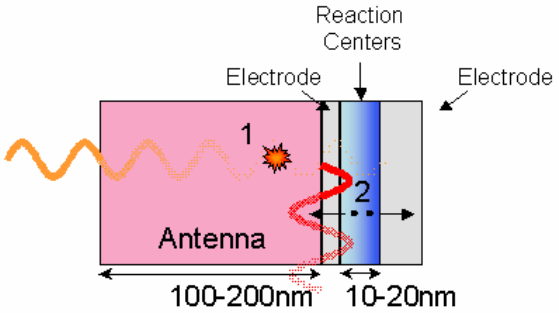

Figure 3: Structure of a PV cell with external antenna. The process begins with the absorption and reemission into surface plasmon polariton (SPP) modes. The oscillating surface fields associated with the SPP couple energy into reaction centers.

To increase the efficiency, we aim to split the electrical and optical functions of solar cells by utilizing an external light absorbing element, as is done in photosynthetic organisms. For this method to be successful, two processes must be efficiently accomplished (see Fig. 3):

(1) Light is absorbed into a solid state antenna. The antenna must then efficiently re-radiate the light into guided optical modes (surface plasmons) created in the thin photovoltaic metal/reaction center/metal stack, thereby effectively transferring energy across the intervening metal electrode.
(2) Energy in plasmon modes propagates perpendicularly to the incident light, and must be efficiently absorbed by the reaction center.

We have simulated the efficiency of surface plasmon absorption in thin film structures in the Otto-Kretschmann configuration using a transfer-matrix method. In this configuration (see Fig. 4), p-polarized light of varying incident angle is coupled through a low index medium. At the resonant angle, the horizontal projection of photon momentum matches that of allowed plasmon modes and energy transfer is allowed. At resonance, the reflected intensity decreases and light absorption in an organic semiconductor increases. The model verifies that light absorption in thin films can increase light absorption significantly; when applied to very thin solar cells, a dramatic increase of several orders of magnitude in efficiency is predicted, from <1% to 80%. We have verified these predictions experimentally in thicker solar cells and observe an increase in efficiency by a factor of 2. Our demonstration of solar cell excitation by plasmons demonstrates the validity of the second process of the external antenna scheme.

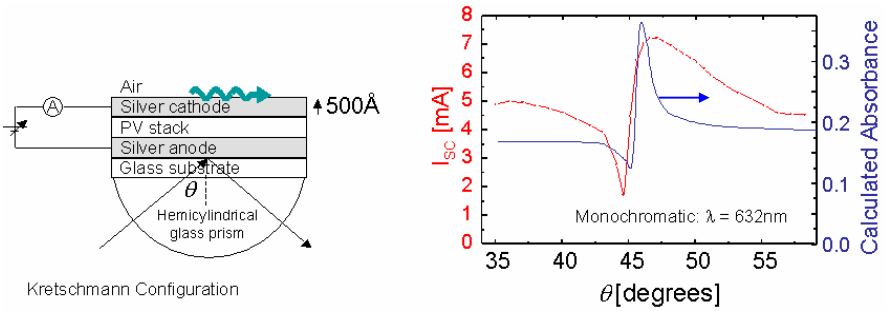

Fig. 4: The solar cell is comprised of evaporated thin films of silver and two organic semiconductors (CuPc and C60) mounted onto hemicylindrical glass prism. The angle of incidence of light is varied and absorption is monitored via the solar cell photocurrent. A comparison between photocurrent and predicted optical absorption verifies SPPs are responsible for current enhancement. The efficiency of this device nearly doubles at resonance.

References

1. R. Das, P.J. Kiley, M. Segal, J. Norville, A.A. Yu, L. Wang, S. Trammell, L.E. Reddick, R. Kumar, S. Zhang, F. Stellacci, N. Lebedev, J. Schnur, B.D. Bruce and M.A. Baldo, "Solid State Integration of Photosynthetic Protein Molecular Complexes," *Nano Letters*. 4: 1079-1083 (2004).

2. P. Kiley, X. Zhao, M. Vaughn, M.A. Baldo, B.D. Bruce and S. Zhang, "Self-assembling Peptide Detergents Stabilize Isolated Photosystem I on a Dry Surface for an Extended Time," *PLoS Biology*. 3: e230 (2005).

2. Fundamental Efficiency Limits of Electroluminescence in Organic Semiconductors

Sponsors
National Science Foundation MRSEC(DMR 02-13282)

Project Staff
Michael Segal, Professor Marc Baldo

Collaborators
Joseph Shinar, Iowa State University; Zoltan Soos, Princeton University

The formation of molecular excited states (excitons) in organic semiconductors determines the maximum achievable efficiency of organic light emitting devices (OLEDs). Excitons are generated in OLEDs from the combination of injected electrons and holes. Since its constituent electron and hole can each be spin-up or spin-down, an exciton can have four different spin states: three states, known as triplet states, have a total spin of one; and the remaining singlet state has a total spin of zero. Many OLED materials, most notably polymeric materials, can only emit light from the singlet state. Thus, in polymeric OLEDs, the fraction of singlet states formed by charge injection determines the fundamental efficiency. Small molecular-weight phosphors, however, allow light emission from all exciton states [1]. Since the burgeoning OLED industry is divided between small-molecular weight and polymeric technologies, determination of the singlet fraction in polymers has become commercially significant since it quantifies the efficiency advantage of small molecular-weight phosphors.

In the simplest model of exciton formation, it follows from counting states that singlets are expected to account for 25% of excitons. Several experimental and theoretical studies have recently suggested, however, that electrical excitation of polymers generates far more than 25% singlet excitons [2-4]. Many of these studies have been based on electron spin resonance (ESR) measurements. Our research in this

area can be divided into two broad categories: (1) formulating a robust method for measuring the spin statistics in an organic luminescent material and applying the method to an archetypal organic polymer in which a high singlet ratio has been measured; and (2) developing a model for the magnetic resonance in organic semiconductors and considering its implications for spin statistics.

Measuring The Singlet Ratio

Fig. 1 shows the method we have developed for measuring the spin statistics in an organic luminescent material [5]. An OLED is fabricated with the material of interest serving as its luminescent layer, and two types of efficiencies are measured. First, the OLED is operated normally, with injected electrons and holes combining to form both singlets and triplets in the ratio χ_S : (1-χ_S). Only the singlets emit light. The ratio of the measured luminescence to the driving current gives the electroluminescent (EL) efficiency. Then, the OLED is operated in reverse bias while exposed to an optical pump, which generates only singlet excitons. The reverse bias electric field breaks some singlet excitons into electrons and holes, producing photocurrent and reducing the photoluminescence (PL) by an amount ΔPL. The ratio of ΔPL to the photocurrent then gives the PL efficiency. The singlet ratio χ_S is then simply the ratio of EL to PL efficiency.

This measurement technique has the advantage that it is a *relative* measurement: because the singlet ratio is derived from a ratio of efficiencies, not every photon must be captured, as in many other measurements. In addition, the shape of the ΔPL versus photocurrent characteristic reveals possible degradation of the luminescent material. A degraded material may otherwise yield artificially high singlet ratios.

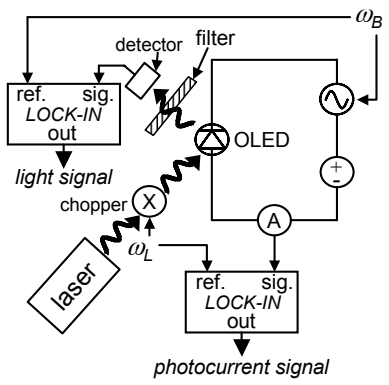

Fig. 1 - The experimental setup of the spin statistics measurement. When the OLED is operated in forward bias, EL is collected by the detector. Spin statistics are determined by comparing the EL to the PL efficiency as determined by photoexciting the OLED under reverse bias. The photocurrent is detected synchronously with the optical chopping frequency, and the PL is locked to the modulation frequency of the reverse bias voltage. This scheme rejects leakage current and optical pump fluctuation.

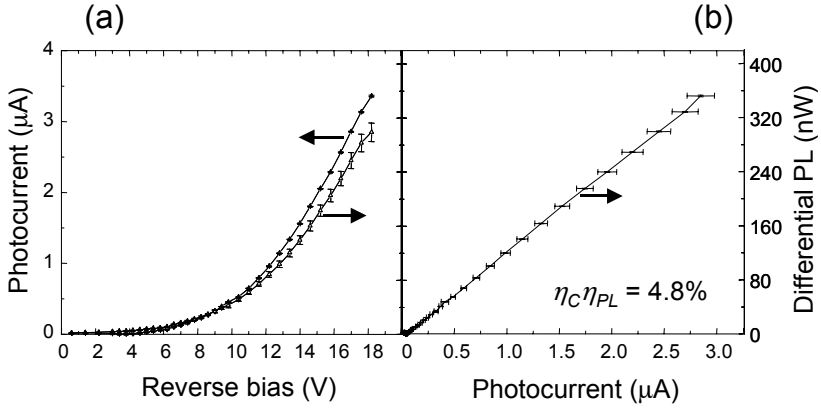

Fig. 2 - **(a)** Synchronously-detected photocurrent and the corresponding decrease in PL for the polymer MEH-PPV as a function of reverse bias. **(b)** The relationship between the decrease in PL and photocurrent gives the synchronously-detected out-coupled PL efficiency.

Applying this technique to the archetypal small molecular weight luminescent material tris(8-hydroxyquinoline) aluminum (Alq_3) yielded a singlet ratio of (20±1)%, in agreement with previous studies [6]. The archetypal luminescent polymer poly[2-methoxy-5-(2-ethylhexyloxy)-1,4-phenylenevinylene] (MEH-PPV) yielded a singlet ratio of (20±4)%, in disagreement with other studies which have found it to be well above 25% [2-3].

Magnetic Resonance and Spin-Dependent Exciton Formation

In ESR measurements, an organic semiconductor is cooled to low temperature and exposed to a continuous optical pump that generates singlet and triplet excitons. Some charges will also be formed by the dissociation of excitons. The charges may be solitary, or they may exist in closely spaced, oppositely charged pairs, so called polaron pairs, which are the precursors for excitons. A magnetic field is applied to split degenerate energy levels of the spin one triplet excitons and spin ½ charges, and a microwave field tuned to this energy splitting causes an equalization of populations. It is experimentally observed that placing an organic semiconductor under resonance conditions increases its PL. The physical model for this behavior has a direct bearing on the question of the singlet ratio: one such model, based on spin dependent exciton formation, predicts high singlet ratios in polymers [2].

We propose instead that the resonant phenomenon results from reduced quenching under resonance. It is well known that triplets and charges (more precisely defined as polarons in these materials) can 'quench' singlets, preventing them from emitting light, and the populations of these quenchers are indeed observed to decrease under resonance. We further propose that the reason for this decrease is an enhanced rate of spin-dependent triplet-polaron collisions. In such a collision, shown schematically in Fig. 3, a triplet collides with a trapped polaron and is quenched. The polaron is excited is then more likely to recombine with an oppositely charged polaron. This collision is allowed only 1/3 of the time out of resonance, but is effectively always allowed in resonance.

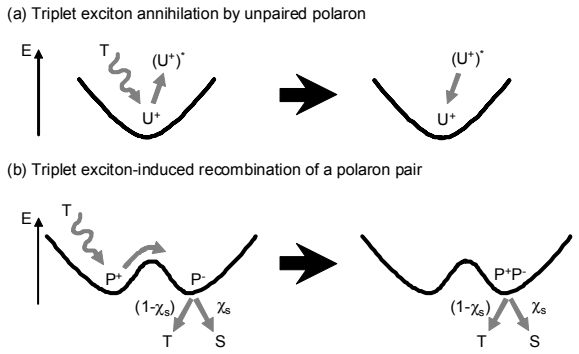

Fig. 3 – Models for collision between a triplet exciton and **(a)** unpaired and **(b)** paired polarons at low temperature. In **(a)**, a TE is annihilated by a solitary polaron. The polaron is excited by the collision but relaxes before it encounters an oppositely charged polaron, and is therefore unaffected by TE-polaron collisions or magnetic resonance. In **(b)**, a pair of oppositely charged polarons is trapped in nearby energy wells. After collision with a triplet exciton, the triplet exciton is annihilated, and one of the polarons is excited, increasing its probability of crossing the energy barrier separating it from its oppositely charged partner.

To test the triplet-polaron-mediated quenching theory, we have conducted a magnetic resonance experiment in which the optical pump was modulated at a rate too high for triplets or polarons to respond, but low enough for singlets to respond [7,8]. The PL was then detected at the optical modulation frequency, and was found to be large and independent of modulation frequency. This data proves that magnetic resonance is a quenching phenomenon and is consistent with the triplet-polaron picture.

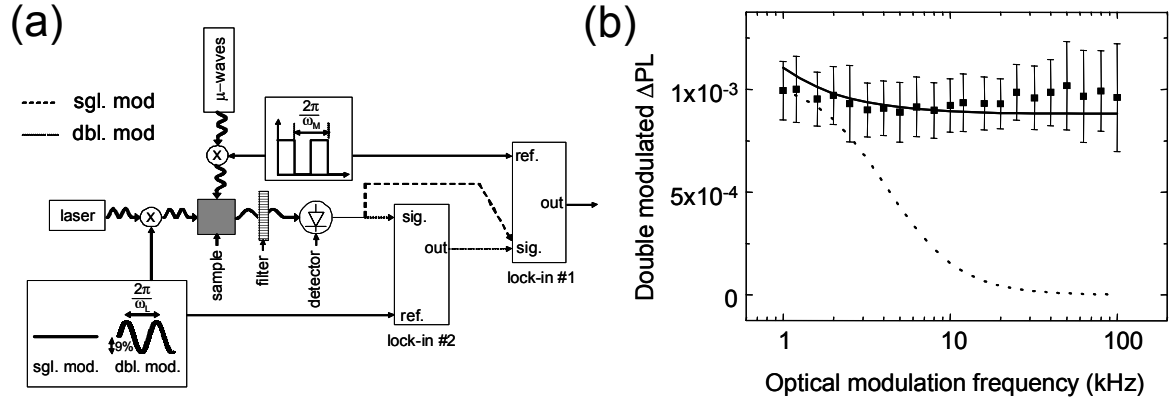

Fig. 4 – **(a)** The experimental setup for measuring the frequency response of the photoluminescence-detected magnetic resonance. The single-modulation result is measured with a single lock-in amplifier and microwave power modulation only, using the dashed signal path. The double-modulation result is measured with two lock-in amplifiers and both laser power and microwave power modulation, using the dotted signal path. **(b)** Double modulation data for the polymer MEH-PPV as a function of laser modulation frequency with the microwave modulation frequency held constant at 200 Hz. The solid and dotted lines are the predictions of the triplet-polaron quenching and spin dependent recombination models respectively.

Conclusion

Together with the recent report by Lupton, et al. [9] that demonstrated that the interchange between singlet and triplet polaron pairs in polymers is extremely slow, our work suggests that exchange effects are significant in polaron pairs. If singlet and triplet polaron pairs are indeed not degenerate as has been supposed, then predicted differences in the formation rate of singlet and triplet excitons will not alter the singlet fraction from 25%. Claims of singlet fractions of > 25% in polymers could be definitively settled by the observation of EL efficiencies approaching those observed in phosphorescent OLEDs. Although polymeric devices typically exhibit larger output coupling fractions since the chains are preferentially aligned in-plane, the absence of high EL efficiencies suggests that the singlet fraction may indeed be close to 25% in polymeric devices.

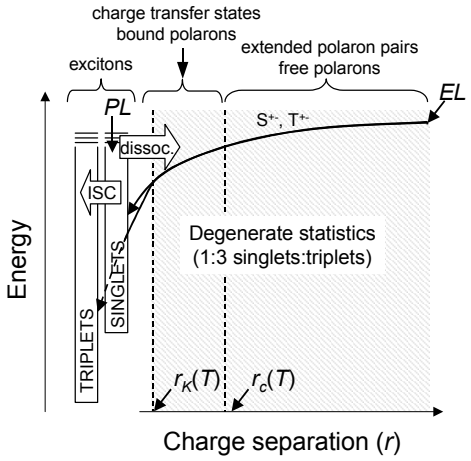

Fig. 5. Injected electrons and holes in organic semiconductors may form either singlet or triplet excitons. At large charge separations, singlet and triplet pair states are degenerate, and it is assumed that there is one singlet pair for every three triplet pairs. Once bound by coulombic interactions, the formation of excitons is mediated by charge transfer (CT) states. But if exchange interactions are significant in the CT states then the singlet fraction will be close to 25%.

References

1. M.A. Baldo, D.F. O'Brien, Y. You, A. Shoustikov, S. Sibley, M.E. Thompson and S.R. Forrest, "High efficiency phosphorescent emission from organic electroluminescent devices" *Nature*. 395: 151-154 (1998).

2. M. Wohlgenannt, K. Tandon, S. Mazumdar, S. Ramasesha and Z.V. Vardeny, "Formation cross-sections of singlet and triplet excitons in pi-conjugated polymers," *Nature*. 409: 494-497 (2001).

3. Y. Cao, I. Parker, G. Yu, C. Zhang and A. Heeger, "Improved quantum efficiency for electroluminescence in semiconducting polymers," *Nature*. 397: 414-417 (1999).

4. J.S. Wilson, A.S. Dhoot, A.J.A.B. Seeley, M.S. Khan, A. Köhler and R.H. Friend, "Spin-dependent exciton formation in pi-conjugated compounds," *Nature*. 413: 828-831 (2001).

5. M. Segal, M.A. Baldo, R.J. Holmes, S.R. Forrest and Z.G. Soos, "Excitonic singlet-triplet ratios in molecular and polymeric organic materials," *Physical Review B*. 68: 075211 (2003).

6. M.A. Baldo, D.F. O'Brien, M.E. Thompson and S.R. Forrest, "The excitonic singlet-triplet ratio in a semiconducting organic thin film," *Physical Review B*. 60: 14422-14428 (1999).

7. M.K. Lee, M. Segal, Z.G. Soos, J. Shinar and M.A. Baldo, "Yield of Singlet Excitons in Organic Light-Emitting Devices: A Double Modulation Photoluminescence-Detected Magnetic Resonance Study," *Physical Review Letters*. 94: 137403 (2005).

8. M. Segal, M.A. Baldo, M.K. Lee, J. Shinar and Z.G. Soos, "The Frequency Response and Origin of the Spin-1/2 Photoluminescence-Detected Magnetic Resonance in a pi-Conjugated Polymer," *Physical Review B*. 71: 245201 (2005).

9. M. Reufer, M.J. Walter, P.G. Lagoudakis, A.B. Hummel, J.S. Kolb, H.G. Roskos, U. Scherf and J.M. Lupton, "Spin-conserving carrier recombination in conjugated polymers," *Nature Materials*. 4: 340-346 (2005).

3. Interface Disorder and Charge Injection into Organic Semiconductors

Sponsors
MARCO Materials Structures and Devices Center

Project Staff
B.N. Limketkai, M.A. Baldo

Charge injection dominates the electrical properties of almost every organic electronic device. But the temperature and electric-field dependence of charge injection from metals into films of organic semiconductors has, to date, resisted description by analytic theories.[1] In this project, we examine the effect of structural disorder at the injection interface on the current-voltage (IV) characteristics of organic semiconductors. We find that structural disorder at the injection interface creates energetic disorder with a variance that is typically several tenths of an eV. Thus, structural disorder effectively generates deep interface traps that are observed to dominate the IV characteristics of these materials. For example, ultraviolet photoelectron spectroscopy data taken by Peisert, *et al.*[2] in Fig. 1 shows the effect of structural disorder on the energetic disorder of the highest occupied molecular orbitals (HOMOs) of copper phthalocyanine on gold surfaces.

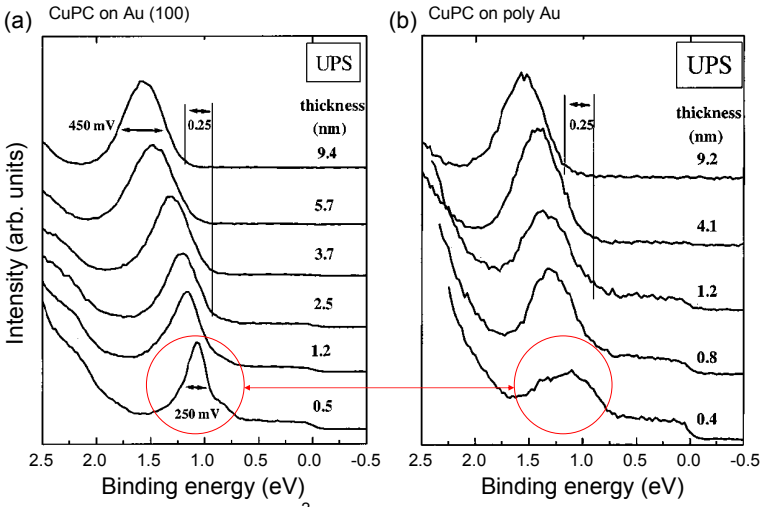

Fig. 1. Data of Peisert, et al.[2] showing significant differences in the width of the HOMO of CuPC on flat and rough Au substrates.

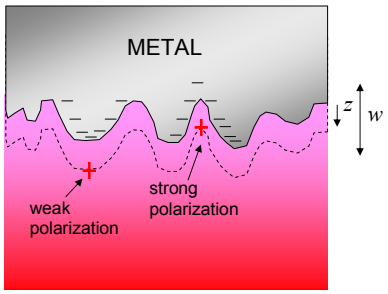

Fig. 2. The geometry of the image charge calculation at a rough interface.

Calculations of interfacial disorder

For metal electrodes, interfacial energetic disorder is due primarily to variation in the image charge effect on a rough metal surface. Modeling the metal surface as self-affine, *i.e.* fractal over a proscribed range of length scales, we find that the standard deviation in the energy levels of the semiconductor is:[3]

$$\sigma(z_0) \approx \frac{q^2}{8\pi\varepsilon_r\varepsilon_0}\frac{w}{z^2}.$$

where z is the distance of the charge from the metal interface, w is the global rms roughness of the metal interface, q is the electron charge and $\varepsilon_r\varepsilon_0$ is the permittivity. Most notably, for equally spaced molecular layers, the $1/z^2$ decay of the energetic disorder yields the ratio of standard deviations of energy levels in the first and second molecular layers:[3]

$$\sigma_1/\sigma_2 = 4.$$

σ_1 and σ_2 are the standard deviation of transport states in the first and second layers, respectively. This result is *independent* of material parameters such as the surface roughness. Since the image charge effect at an ideal flat interface scales as $1/z$, the $1/z^2$ dependence of energetic disorder at a rough interface may be understood as the first perturbation of the image charge effect.

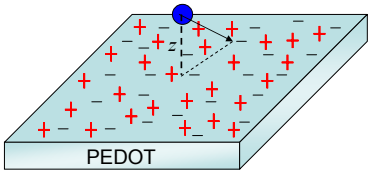

Fig. 3. The charged surface of PEDOT is disordered.

There are other causes of energetic disorder at interfaces in addition to the image charge effect. For example, poly(3,4-ethylenedioxythiophene):poly(4-styrenesulphonate) (PEDOT:PSS), a densely charged polymer used frequently as an injection interface, is not expected to exhibit strong image charge effects, but the charge distribution on the PEDOT surface is expected to be disordered. Recently, we have generalized the interfacial disorder calculation to include non-metallic interfaces such as PEDOT. We found that the $1/z^2$ dependence is also expected at these highly charged polymer interfaces.

Analytic model of charge injection at a disordered interface

When electrical bias is applied to a disordered metal-organic interface, the voltage determines the quantity of charge trapped in the interface states. The current density is determined by the rate of charge hopping from the interfacial layer to less disordered sites in the second molecular layer.[4] Using the Marcus expression for charge hopping between Gaussian distributions gives a master equation:[3]

$$J = J_0 \left(V + \Delta V\right)^m \Big/ V_0^m$$

where ΔV is the doping-dependent voltage shift, and J_0 and V_0 are constants. ΔV contains the entire cathode dependence of injection; it is equivalent to the additional voltage required to inject an amount of charge equal to the doped charge present in the boundary layer. The power law slope, $m = 1 + \sigma_1^2 \Big/ \left(\sigma_2^2 + 2\lambda kT\right)$, where λ is the reorganization energy of the molecule. At low temperatures, the decay of energetic disorder gives $m = 1 + \sigma_1^2 / \sigma_2^2 \approx 17$.[3]

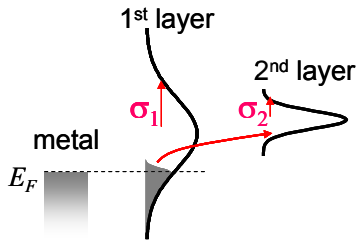

Fig. 4. Charge injection when dominated by interface traps.

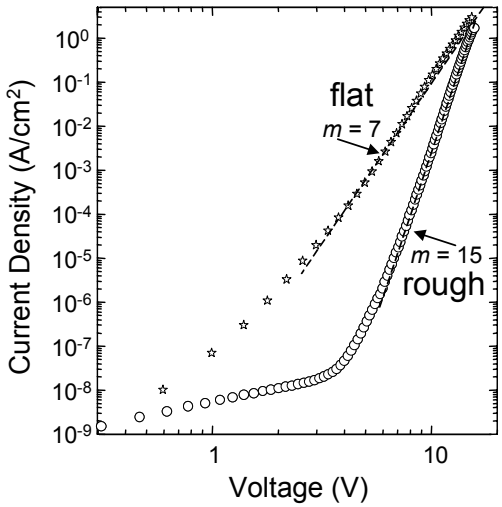

Fig. 5. A comparison between the *IV* characteristics of rough and atomically flat gold injecting contacts to CuPC at T=10K.

Experimental Data

The low temperature IV characteristics of CuPC on flat gold, and rough gold is shown in Fig. 5. The CuPC on rough gold is a highly resistive contact, with a power law slope of m = 15. CuPC on flat gold, however, is significantly more conductive, and its power law is only m = 7. Thus, CuPC on rough gold behaves as expected given the large density of traps at its structurally disordered injection interface.

To demonstrate the universality of the model, the IV characteristics of a wide variety of electron injection contacts are shown in Fig. 6. The power law slope is m = (20±1) at 10K, independent of the choice of cathode or organic material, demonstrating that electron injection at these interfaces is not controlled by an energy barrier between the metal and organic semiconductor.

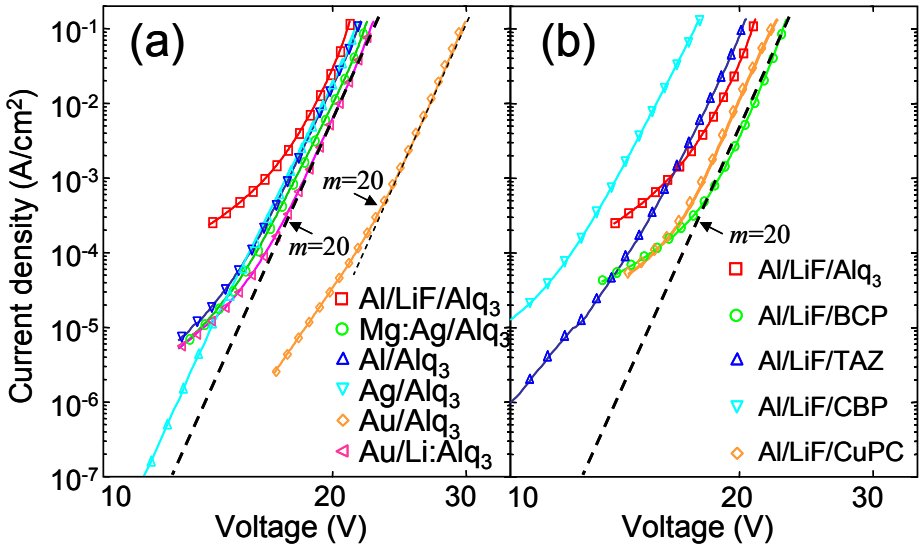

Fig. 6. The IV characteristics at T = 10K for **(a)** Alq_3 interfaces, and **(b)**, a comparison of Al/LiF contacts to Alq_3, BCP, TAZ, CBP, and CuPC. All cathodes exhibit similar power law behavior, i.e. $J \sim V^m$, where m = (20±1).

In Fig. 7 we plot the temperature dependence of the IV characteristics for a variety of cathodes on Alq_3. If we assume that ΔV contains the cathode dependence, then we expect that all the IV characteristics should be related by rigid shifts in voltage. This is confirmed in Fig. 7.

Finally, in Fig. 8, we plot the temperature dependence of ΔV for different cathodes. The temperature dependence of the rigid voltage shift ΔV is observed to fit:[3]

$$\Delta V = \Delta V_0 + \left(qa_0 d / \varepsilon_r \varepsilon_0\right) N_D \exp\left[-E_A / kT\right]$$

where E_A is the activation energy, and ΔV_0 is a temperature-independent constant determined by the equilibrium density of charge in the LUMO states at zero temperature. Assuming that ΔV is due to cathode-induced doping of the interfacial states, N_D is assigned as the effective doping density.

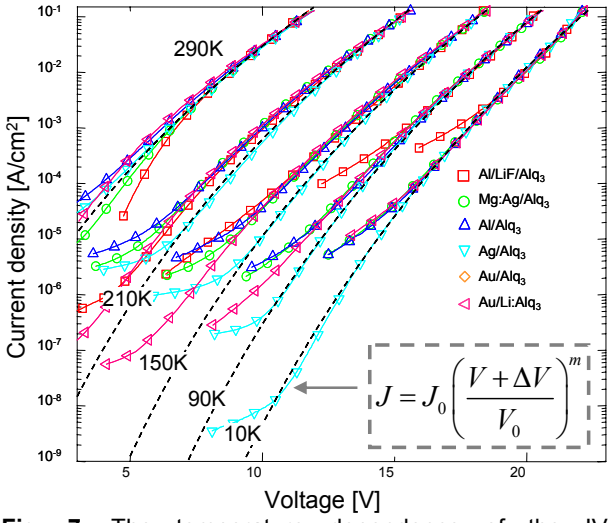

Fig. 7. The temperature dependence of the IV characteristics of Alq_3 interfaces. A rigid voltage shift was applied to the Alq_3 characteristics to overlap with the Mg:Ag/Alq_3 data. The $\Delta V = 0$ fit is shown in dotted lines for each organic material.

Since the activation energy of ΔV is observed to be much less than the energetic disorder at the interface, we speculate that E_A is determined by the temperature dependence of charge diffusion. From the Marcus charge hopping expression, the temperature dependence of the isoenergetic diffusion constant, D, is described by:

$$D \propto \kappa \exp\left[-\lambda / 4kT\right]$$

For fitted values of the molecular reorganization energy $\lambda \approx 160$ meV, $E_A \approx \lambda/4$, consistent with the diffusion hypothesis.[3]

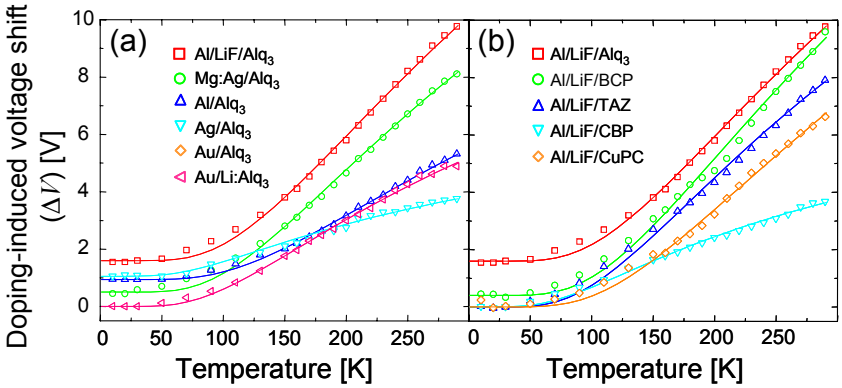

Fig. 8. The temperature dependence of doping for **(a)** Alq_3 interfaces, and **(b)**, a comparison of Al/LiF contacts to Alq_3, BCP, TAZ, CBP, and CuPC. In all cases, the temperature dependence of doping is found to follow Arrhenius behavior.

Conclusion

We have demonstrated that interfacial disorder is an important determinant of the IV characteristics of organic semiconductor injection contacts. Interfacial disorder creates traps, which may be recognized by power law IV characteristics. Since very few practical organic semiconductor devices employ atomically flat injection contacts, we expect that the theory is generally applicable to organic devices.

References

1. J.C. Scott, "Metal-organic interface and charge injection in organic electronic devices," *Journal of Vacuum Science and Technology A*. 21: 521-531 (2003).

2. H. Peisert, M. Knupfer, T. Schwieger, J.M. Auerhammer, M.S. Golden and J. Fink, "Full characterization of the interface between the organic semiconductor copper phthalocyanine and gold," *Journal of Applied Physics*. 91: 4872-4878 (2002).

3. B.N. Limketkai and M.A. Baldo, "Charge injection into cathode-doped amorphous organic semiconductors," *Physical Review B*. 71, 085207 (2005).

4. M.A. Baldo and S.R. Forrest, "Interface limited injection in amorphous organic semiconductors," *Physical Review B*. 64: 085201 (2001).

Journal Publications, Published

M. Segal, M.A. Baldo, M.K. Lee, J. Shinar and Z.G. Soos, “The Frequency Response and Origin of the Spin-1/2 Photoluminescence-Detected Magnetic Resonance in a pi-Conjugated Polymer,” *Physical Review B*. 71: 245201 (2005)

M.K. Lee, M. Segal, Z.G. Soos, J. Shinar and M.A. Baldo, “On the Yield of Singlet Excitons in Organic Light-Emitting Devices: A Double Modulation Photoluminescence-Detected Magnetic Resonance Study,” *Physical Review Letters*. 94: 137403 (2005)

P. Kiley, X. Zhao, M. Vaughn, M.A. Baldo, B.D. Bruce and S. Zhang, “Self-assembling Peptide Detergents Stabilize Isolated Photosystem I on a Dry Surface for an Extended Time” *PLoS Biology*. 3: e230 (2005)

B.N. Limketkai and M.A. Baldo, “Charge injection into cathode-doped amorphous organic semiconductors,” *Physical Review B*. 71: 085207 (2005)

R. Das, P.J. Kiley, M. Segal, J. Norville, A.A. Yu, L. Wang, S. Trammell, L.E. Reddick, R. Kumar, S. Zhang, F. Stellacci, N. Lebedev, J. Schnur, B.D. Bruce and M.A. Baldo, “Solid State Integration of Photosynthetic Protein Molecular Complexes,” *Nano Letters*. 4: 1079-1083 (2004)

M.A. Baldo and M. Segal, “Phosphorescence as a Probe of Exciton Formation and Energy Transfer in Organic Light Emitting Diodes,” *Physica Status Solidi A*. 201: 1205-1214 (2004)

M. Segal and M.A. Baldo, “Reverse bias measurements of the photoluminescent efficiency of semiconducting organic thin films,” *Organic Electronics*. 4: 191-197 (2003)

M. Segal, M.A. Baldo, R.J. Holmes, S.R. Forrest and Z.G. Soos, “Excitonic singlet-triplet ratios in molecular and polymeric organic materials,” *Physical Review B*. 68: 075211 (2003)

Book Chapters

M.A. Baldo and M. Segal, “Phosphorescence as a probe of exciton formation and energy transfer*,”* in *Physics of Organic Semiconductors*, edited by W. Brütting. (Wiley VCH, 2005).